# Plantar soft tissue loading under the medial metatarsals in the standing diabetic foot

Amit Gefen *

*Department of Biomedical Engineering, Faculty of Engineering, Tel Aviv University, Tel Aviv 69978, Israel*

## Abstract

Diabetes mellitus (type 2) is the most frequent cause of non-traumatic lower-limb amputations. The major cause of impairment to the feet of diabetics is persistent hyperglycemia, potentially leading to peripheral neuropathy as well as to pathological changes in plantar soft tissue, which stiffen its structure and diminish its ability to effectively distribute foot–ground contact loads. In this study, a computational model of the foot structure in the standing position was utilized to evaluate stress distributions in plantar soft tissue under the medial metatarsal heads of simulated diabetic versus normal feet. The model comprises five anatomic planar cross-sections in the directions of the foot rays, which were solved for internal stresses under static ankle joint reaction (300 N) and triceps surae muscle forces (150 N) using the finite element method. Tissues were assumed to be homogenous, isotropic and elastic materials, with nonlinear stress-strain relations for the ligaments, fascia and plantar tissue. The model revealed significant tension stress concentrations (90–150 KPa) in the plantar pad of the simulated diabetic forefoot: they were four times the normal maximum stress under the first metatarsal head and almost eight times the normal maximum stress under the second metatarsal head. It was shown that with increased severity of stiffening of the plantar pad, as related to glucose-exposure, peak forefoot contact stresses may rise by 38 and 50% under the first and second metatarsal heads, respectively. The increase in averaged (von Mises) internal stresses within the plantar soft tissue is even more pronounced, and may rise by 82 and 307% for the tissue under the first and second metatarsal heads, respectively. These results, which conform to experimental data gathered over the last two decades, suggest that the process of injury in diabetic feet is very likely to initiate not on the skin surface, but in deeper tissue layers, and the tissues underlying the distal bony prominences of the medial metatarsals are the most vulnerable ones.
© 2003 IPEM. Published by Elsevier Science Ltd. All rights reserved.

*Keywords:* Biomechanical model; Plantar pressure; Diabetes mellitus; Therapeutic footwear; Finite element method

## 1. Introduction

About 60–70% of the diabetic patients suffer nerve damage as a result of the disease. The severe form of diabetic nerve damage can lead to lower-limb amputations and in fact, diabetes mellitus (type 2) is the most frequent cause of non-traumatic lower-limb amputations. Current statistics show that the risk of a limb amputation is 15–40 times greater for a diabetic patient and that in the United States, 82,000 people lose their foot or leg due to diabetes each year (American Diabetes Association, 'Facts & Figures', www.diabetes.org). The basic cause of diabetic foot injury is hyperglycemia. Hyperg-lycemia induces metabolic derangements that directly affect the Schwann cells (myelin) and nodes of Ranvier (axons). Hyperglycemia may also affect the structure and function of endoneurial microvessels, thereby altering the blood-nerve barrier and causing local hypoxia or ischemia [1]. This potentially leads to peripheral sensory neuropathy, which evolves in about 25% of adult diabetic patients [2–4]. Peripheral sensory neuropathy disables the protection (pain) mechanism that is normally activated when the plantar soft tissue is damaged.

Increased stiffening of collagen-rich soft tissues has also been noted in diabetes [5,6]. A number of studies identified alterations in collagen structure and function as related to the glucose-exposure. The abnormalities included increased fibril diameter, closer packing of fibrils and irregular fibril shapes (indicating local fusion of adjacent fibrils). Important findings are that cross-

* Tel.: +972-3-640-8093; fax: +972-3-640-5845.
*E-mail address:* gefen@eng.tau.ac.il (A. Gefen).

linking of adjacent collagen fibrils and nonenzymatic glycosylation of keratin occur with the glycation [7,8], causing substantial stiffening of the affected tissues, including hyperkeratosis and formation of thickened callus in the plantar skin [9,10]. This mechanism has an overall effect of mechanically stiffening the plantar diabetic tissue, whereupon soft tissue that pads the metatarsal heads becomes less elastic and less able to distribute pressure through deformation [11–13]. Hence, the overall 'cushioning' property of the plantar soft tissue, especially at high-pressure sites such as those under the medial metatarsals, is damaged.

The heads of the medial metatarsals were shown to transfer extensive foot-ground contact forces during both standing and gait (see Ref. [14] for a review). It follows that pathologic stiffening of the plantar soft tissue that pads the medial metatarsals may cause stress concentrations, which could lead to micro-tears in the tissue during load bearing (microscopic tears in tissue, formed when there is sufficient stress placed on the tissue to lead to local ruptures), especially when improper footwear is used [11]. These minor wounds, unnoticed by the neuropathic patient, may develop into ulcers and, in severe cases, may be infected and require lower-extremity amputations [3,4]. Clinical studies have indicated that in order to fully determine the level of risk for diabetes-related foot ulceration, both static (standing) and dynamic (gait) measurements of the plantar pressures are required [15,16].

The mechanical interaction between the foot and supportive surfaces can be studied both experimentally and numerically. While experimental analyses of foot-ground or foot-shoe contact are limited solely to measurements of interfacial pressures, a reliable numerical model can provide both the interfacial pressures and some insight into internal stresses tolerated by the plantar tissue [17]. Several recent models have used the finite element (FE) method to predict the loading of the foot's components during standing and gait as they relate to foot disorders and therapeutic footwear. Chu et al. [18] presented an asymmetric three-dimensional FE model for analysis of the effects of ankle-foot orthoses. Patil et al. [19] used a two-dimensional model that had been constructed according to a lateral X-ray image in order to study stress distributions in normal and neuropathic feet. Lemmon et al. [20] used FE simulations of an isolated second metatarsal and underlying soft tissue to study effects of insole geometry on the relief of pressure. Nevertheless, changes in stress distributions within the plantar soft tissue under the medial metatarsals in the diabetic foot have not been investigated. In the present study, a computational model of the foot structure in the standing posture [21] was utilized to evaluate the distribution of stresses in the plantar soft tissue under the medial metatarsal heads of simulated diabetic versus normal feet, based on recently published experimental findings [13].

## 2. Methods

Obtaining the stresses in soft tissues above the high-contact-pressure sites during standing, especially under the medial metatarsal heads where injury is common, is a fundamental step towards dynamic stress analyses of the diabetic foot. While foot-ground contact pressures and internal foot stresses are considerably higher during gait compared with standing [14], the loading system acting on the walking diabetic foot is much more complex, and should be investigated separately. Hence, this first study was designed to provide insight on the mechanical behavior of the diabetic plantar pad during the most basic functional posture—standing. The progress of diabetes is represented herein by stiffening the plantar pad of the foot model due to glycation but not by modifying the foot's structure or the standing pattern (as may occur in advanced stages of the diabetic injury). This decision was taken in order to focus the investigation on the pre-injury conditions, and isolate the role of tissue stiffening. The foot model used here to calculate the stress distribution in the plantar neuropathic tissue is described in detail elsewhere [21]. For better understanding of its application to diabetic feet, its essential components are described below.

The model comprises five planar longitudinal cross-sections through the foot, which together yield a convenient representation of its complex half-dome shaped structure (Fig. 1). The geometric data of the foot's skeletal cross-sections of an adult female were detected using magnetic resonance imaging (MRI) and transferred to a commercial FE analysis software package (ANSYS) for construction of planar models for the five rays of the foot. Cartilage layers and ligaments were introduced in the joints based on anatomic data [21]. Bony elements and cartilage were assigned as having the properties of linear, elastic and isotropic materials, while ligaments, fascia and the soft tissue fat pad were considered as being non-linear materials. Young's modulus and Poisson ratio for bone were taken as being 7300 MPa and 0.3, respectively [22], and as 10 MPa and 0.4, respectively, for cartilage [19]. The typical experimental nonlinear stress-strain relations for the ligaments and the plantar fascia were taken according to Race and Amis [23]. For the soft tissue pad, the stress-strain behaviour provided by Nakamura et al. [22] was utilized. These stress-strain data for the ligament/fascia and plantar pad were fitted to polynomial expressions of the fifth-order, of the form
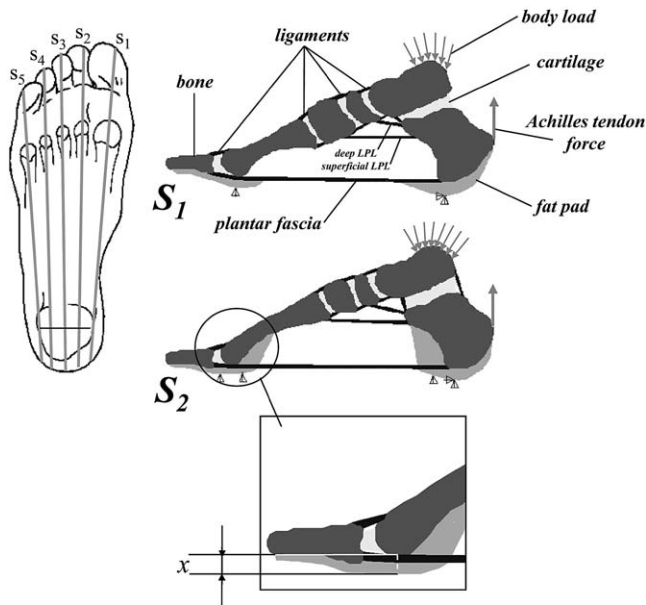
$$\sigma = \sum_{i=0}^{5} c_i \lambda^i \tag{1}$$

Fig. 1. The finite element model of the foot during standing: the five selected planar cross-sections (marked as $S_1$–$S_5$) presented from plantar view (left) and the cross-sectional geometry of the two medial ($S_1$, $S_2$) rays (right). Arrows indicate body loads and forces in the Achilles tendon while standing. The constraints limiting vertical displacements of the plantar surface are marked by triangles. The geometry of the plantar pad under the second metatarsal is magnified to mark the course $x$ for calculation of average stress. LPL = long plantar ligament.

where $\sigma$ is the tissue stress resulted by a stretch ratio $\lambda$, and the constants $c_i$ are as given in Ref. [21].

The literature contains only a small volume of reports concerning mechanical properties of the human foot's tissues, with the least amount of information pertaining to the foot's ligaments. It was stated that the elastic modulus of most ankle ligaments is under or around 200 MPa [24]. For the anterior tibiofibular ligament, uniaxial tension tests resulted loads of ~20 N for 5% strain and ~50 N for 10% strain [25]. The stress-strain relation that was presently assumed for ligaments provides a tangent elastic modulus of 79 MPa at 5% strain and 98 MPa at 10% strain, i.e. intermediate values in terms of the ankle ligament's elastic moduli. Using the same relation, a ligament of the foot with a typical cross-sectional area of 3.2 mm$^2$ (e.g. bundles of the plantar ligaments [21]) is predicted to bear tension of 13 N at 5% strain and 32 N at 10% strain, values which reasonably conform the loads transmitted through the anterior tibiofibular ligament for the same strains. It is hence concluded that the ligament stress-strain data by Race and Amis [23] can be used to represent the mechanical behaviour of the foot ligaments for the purpose of numerical modeling.

The Poisson ratios were taken as 0.4 for the ligaments and fascia and as 0.49 for the soft tissue pad. The model was solved while assuring that (i) ligaments carried only tension stresses and that (ii) no tensile stresses were placed upon the cartilaginous layer beneath bone-cartilage contact regions.

The total load carried by the foot model was determined to be 300 N, which were distributed as 25-19-19-19-18% for the first through the fifth rays, respectively [26]. In addition to the body-weight surface load, a concentrated force of 30 N was applied at the posterior aspect of the calcaneus in each cross-section to represent contraction of the triceps surae muscles during standing [26]. Supports constraining the model's vertical displacements were positioned under the calcaneal base, under each of the five metatarsal heads and under the lateral metatarsal and cuboid bodies.

The FE method was selected for stress analysis of the diabetic foot because of its ability to deal with complex structures of irregular geometry, complex loading and nonlinear material stress-strain relations. The automatic meshing feature of the ANSYS FE pre-processor was employed to create fine meshes of 1100–2000 planar 8-node elements per cross-section of the foot. Optimal meshes were determined by gradually increasing the density of elements and subsequently calculating the internal stress distribution, until maximal differences between succeeding von Mises stress predictions did not exceed 5%. This process was completed for all five cross-sections of the foot rays. The elements selected for the analysis are compatible with large strains, and allow horizontal and vertical translations of each of their eight nodes, to account for bending-related stresses and deformations.

The FE analysis resulted in the distributions of principal tension, principal compression, and the von Mises stresses, as well as the deformations of the foot rays in the standing posture (Fig. 2). Model predictions of percentage of foot-ground reactions carried by the forefoot, midfoot and hindfoot segments of a normal foot were compared with measurements acquired from 20 feet of healthy subjects. No significant differences were indicated by a $t$-test, using the standard 5% level of significance [21].

In the present study, the preceding model was employed for analysis of the effects of diabetic stiffening of the plantar pad on its stress state during standing. In order to simulate the stress distribution within the plantar soft tissue of diabetic patients, we used the recent experimental results of Gefen et al. [13] who demonstrated a substantial increase of plantar soft tissue stiffness in diabetics. Evaluation of local plantar tissue's elastic moduli was achieved through delicate indentation of a rigid pin with a spherical tip into the plantar tissue, which was simultaneously scanned by MRI. The indentation force was acquired using a photoelastic technique (which represents force readings by optical fringes), while tissue deflection was measured on the MRI scans, to yield characteristic load-displacement curves. Measurements were taken for the plantar tissue volumes contained between the first and second metatarsal heads and between the second and third metatarsal heads.
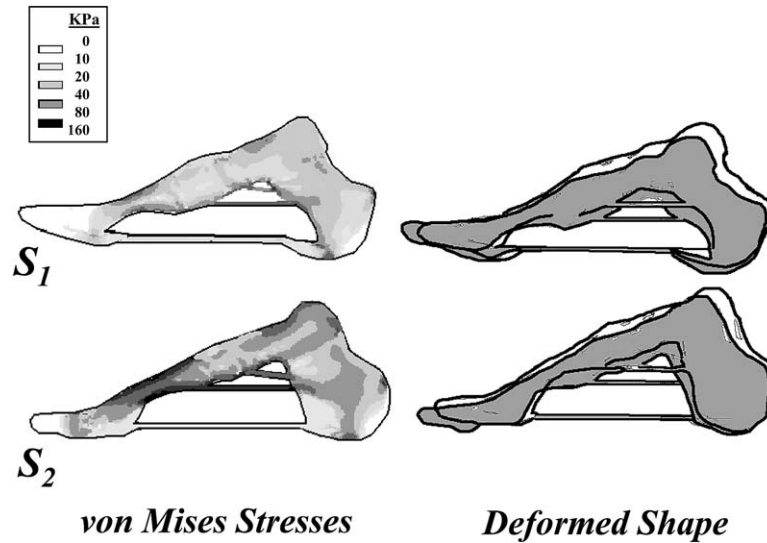
Fig. 2.   Computer simulations of the normal structural behaviour of the foot's medial rays during standing: the distribution of von Mises equivalent stresses in the first and second rays (left) and the deformed shape of their structure (right). The extent of deformation was magnified by a factor of 15 for clarity.

Informed consent was obtained from two healthy subjects (male, 24 yrs old, female, 26 yrs old) and two patients with diabetes mellitus type 2 (males, 72 and 84 yrs old) by the medical staff of Sheba Medical Center, Tel-Hashomer, Israel, where measurements took place. Diabetic patients were pre-assed as being naturopathic. Measurements of plantar tissue elasticity were taken locally for plantar surfaces that appeared to be undamaged, and hence, debridement of callus was not required. The slopes of the curves obtained from the diabetic patients in this study [13] were considerably greater, i.e., five to six times the values obtained from normal subjects. Based on these findings, it was assumed that in a condition representing an advanced stage of diabetes, the stresses required to induce a given strain of the plantar soft tissue are five times greater than those in the normal plantar soft tissue.

In order to simulate progression of the disease, a 'tissue stiffness ratio', $\kappa = \sigma_d(\varepsilon)/\sigma_n(\varepsilon)$, was defined. The ratio $\kappa$ equals the factor of stiffening of the diabetic plantar tissue's stress-strain relation, $\sigma_d(\epsilon)$, in respect to the normal one, $\sigma_n(\epsilon)$, so that its value may range from 1 (normal tissue) to 5 (progressive glycation and stiffening of the plantar pad, due to collagen-cross linking and non-enzymatic glycosylation of keratin). For the purpose of characterizing the loads tolerated by the plantar tissue as the disease progresses, averaged values of the von Mises equivalent stresses distributed over the plantar pad's thickness were examined. The von Mises equivalent stress, $\sigma_{v.M.}$, weighs the effects of principal tension ($\sigma_1$) and principal compression ($\sigma_2$) stresses according to the relation

$$\sigma_{v.M.} = (\sigma_1^2 + \sigma_2^2 - \sigma_1\sigma_2)^{1/2}. \tag{2}$$

As mentioned above, the FE analysis of the foot is focused on the stress distribution in the plantar pad under the first and second metatarsals. These tissues carry most of the forefoot load during standing and gait [14], and are considered the most vulnerable sites for diabetic ulceration [27]. Since deformation of the plantar tissue under the metatarsal heads varies among the different cases, we defined the mean von Mises stress at the plantar pad, $\bar{\sigma}$, as

$$\bar{\sigma} = \frac{1}{x}\int_0^x \sigma_{v.M.}d\xi \tag{3}$$

where the value of $\bar{\sigma}$ averages the von Mises stresses ($\sigma_{v.M}$) over a linear course of length $x$, which originates at the lower plantar part of the metatarsal head, crosses the plantar fascia and the plantar soft tissue throughout their thickness, and terminates at the contact surface with the supports (as indicated in Fig. 1).

## 3. Results

The structural stress distribution (principal and von Mises stresses) in the plantar soft tissue under the medial metatarsals was analyzed for simulations of diabetic versus normal conditions, and the results are shown in Figs. 3 and 4 for the plantar pad under the first and second metatarsal heads, respectively. The tension stresses that developed during the standing posture in the plantar pad underlying the metatarsal heads are shown to be transferred mainly via two mechanisms (see Fig. 3a and 4a): (i) stretching of the plantar fascia under the body weight, which causes local tension proximally to the metatarsophalangeal joints, and (ii) bending of the metatarsal bones, causing tension stresses at their dorsal aspect to
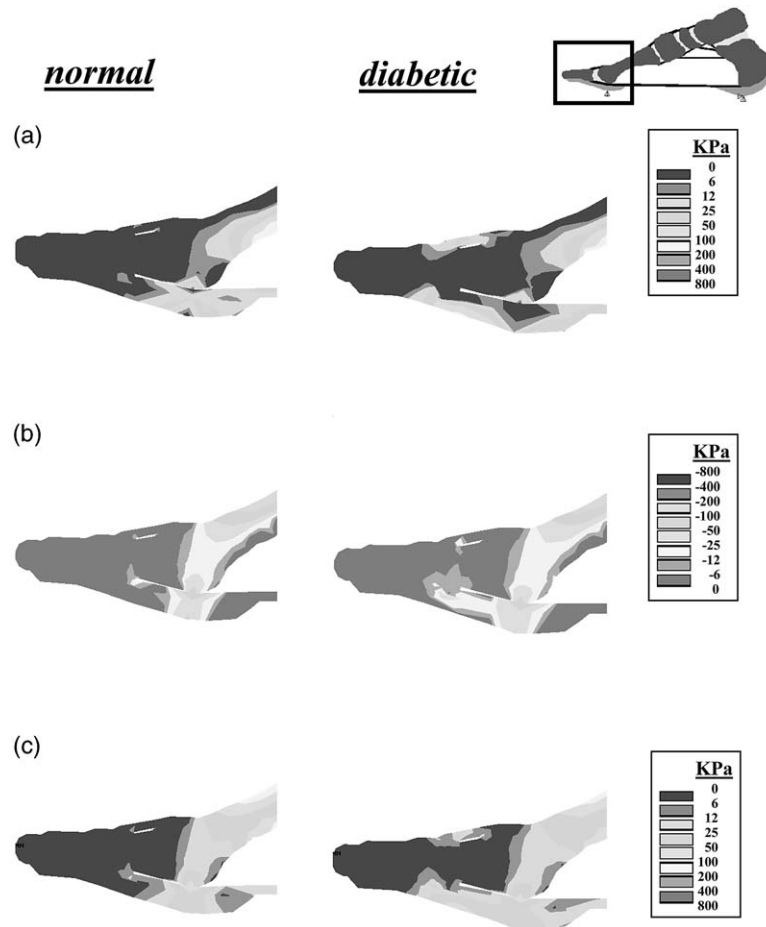
Fig. 3. Diabetic versus normal stress distributions in the plantar pad under the first metatarsal head: (a) principal tension stress, (b) principal compression stress, and (c) von Mises equivalent stress.

flow downward, distally to the metatarsophalangeal joint. The compression stresses generated in the metatarsal bones due to bending under the body load flow downward, through the central and plantar parts of the metatarsals, causing concentrated stresses to generate near the plantar skin under the metatarsal heads.

Examination of the principal stress distribution in simulated diabetic feet revealed significant tension stress concentrations (90–150 KPa) in plantar skin and deeper soft tissues under the metatarsal heads, near the metatarsophalangeal joints. These tension-induced stress concentrations in the tissue of a simulated diabetic foot, which do not appear in the normal foot model, are four times the normal maximum stress under the first metatarsal head and almost eight times the normal maximum stress under the second metatarsal head. Compression stresses also increased substantially in the simulated diabetic foot, reaching peaks of 76 and 99 KPa on the plantar surfaces under the first and second metatarsal heads, respectively. Fig. 5 shows the rise in peak contact pressures and in averaged internal tissue stresses with increasing severity of diabetic stiffening of the plantar pad, in terms of the 'tissue stiffness ratio', $\kappa$. Both peak contact

pressures and averaged internal tissue stresses appear to increase nearly linearly with rise in stiffness of the plantar tissue while $\kappa \leq 4$. It was shown that with greater severity, peak contact stresses may rise by up to 38 and 50% under the first and second metatarsal heads, respectively, when the tissue stiffness ratio $\kappa$ of the plantar pad was increased from a normal value of 1 to a pathologic value of 5 (Fig. 5a). The increase in averaged internal stresses within the plantar pad is even more pronounced. The internal tissue stresses may be elevated by as much as 82 and 307% for the first and second metatarsal heads, respectively (Fig. 5b). This rise is mainly related to the focal tension in deeper soft tissue layers (e.g., see Fig. 4a), which also causes internal shear, proximal to the skin. Both contact stresses and internal tissue stresses grow exponentially with stiffening of the plantar tissue (with a correlation coefficient of 0.94–0.96).

## 4. Discussion

The commonly detected foot ulcers in individuals with diabetes occur in plantar skin and soft tissues under the
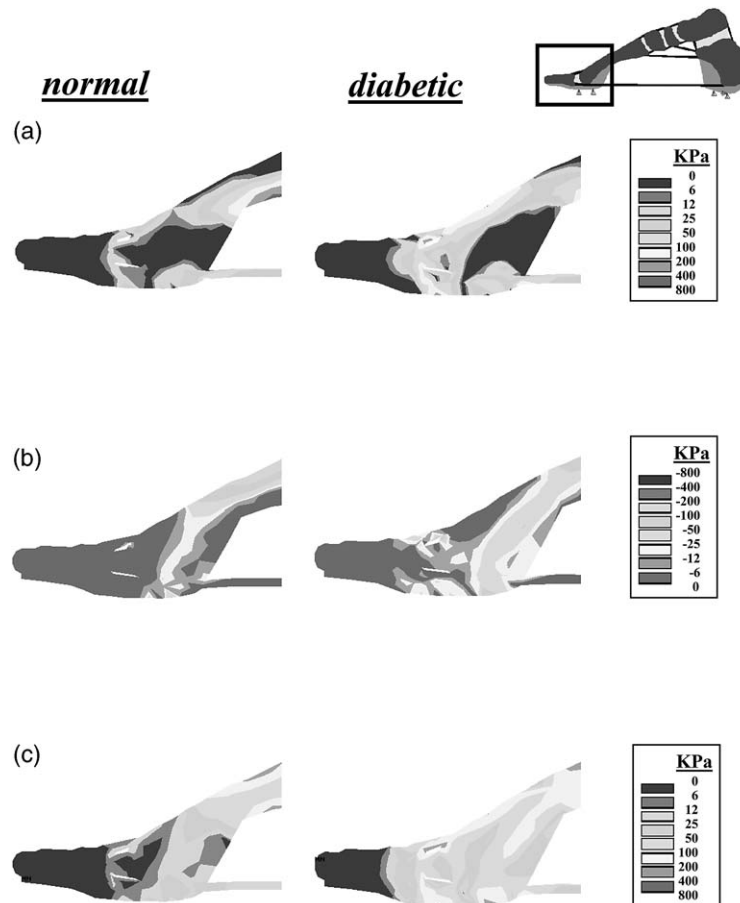
Fig. 4. Diabetic versus normal stress distributions in the plantar pad under the second metatarsal head: (a) principal tension stress, (b) principal compression stress, and (c) von Mises equivalent stress.

first and second metatarsal heads [27]. These are precisely the same locations where the present model predicts significant stress concentrations during standing due to tissue stiffening induced by diabetic glycation. The computational simulations demonstrated that the deeper plantar pad is subjected to a complex loading system, which applies compound stresses with tension, compression and shear components to the soft tissue underlying the metatarsal heads (Fig. 6). It was noted that focal tension of deep soft tissues occurs near the medial metatarsophalangeal joints during standing, and stresses that are up to eight times the normally expected tension value were predicted. It is, therefore, probable that these tension and shear stress concentrations (Fig. 6), which could be expected to increase substantially and become repetitive during gait, cause micro-tears in the diabetic plantar pad. The tears, unnoticed by the neuropathic patients who have lost their 'pain alarm' mechanism, may develop to foot ulceration. Any open lesions will provide a portal of entry for bacteria and infection would occur. This theory of onset and development of injury in the diabetic foot is outlined in Fig. 7. The magnifying effect of stiffening of the plantar tissue on its internal stress levels during load bearing was well demonstrated in this study. The question whether these intensified stress values in diabetic feet are able to produce, through the repetitive application of body loads, micro-tears in the plantar pad that would cause ulceration and/or open a pathway for infection still awaits further studies.

Additional causes of injury, such as poorly fitting footwear or foot deformities (i.e., clawing of the toes) may increase the focal pressures even further and accelerate the development of ulceration. Reduction in toe function and resultant forward migration of some of the cushioning pad of the metatarsal heads, events often observed in diabetics [28,29], are also important factors in the injury process, although, in the absence of quantitative experimental data of reduction in the pad's thickness, they could not be accounted for in the present model. Large-scale statistical studies are still required for quantifying reduction in plantar tissue thickness and related geometrical changes in diabetic feet through the course of the disease.

The investigation of plantar pressures in the standing posture is simpler than dynamic analyses. Most of the available literature documents the dynamic pressures under the foot and their evolution throughout the stance
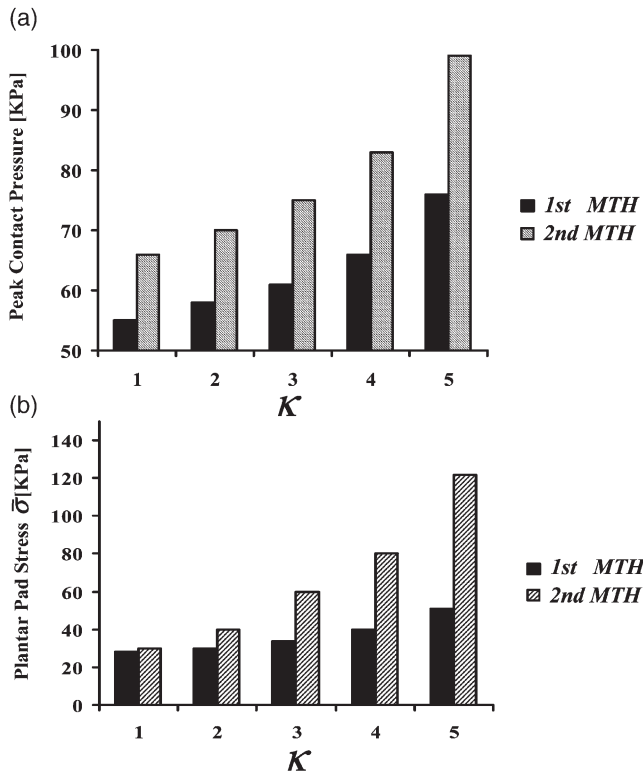
(a)



(b)



Fig. 5. Model predictions of (a) peak contact stresses at the foot-ground interface and (b) averaged internal (von Mises) tissue stresses over the plantar pad thickness under the medial (first and second) metatarsals. Contact and internal stresses are plotted for different stages of tissue stiffening caused by diabetic-induced protein glycation. The level of pathological stiffening of the plantar pad is expressed in terms of the 'tissue stiffness ratio', $\kappa$. MTH= metatarsal head.
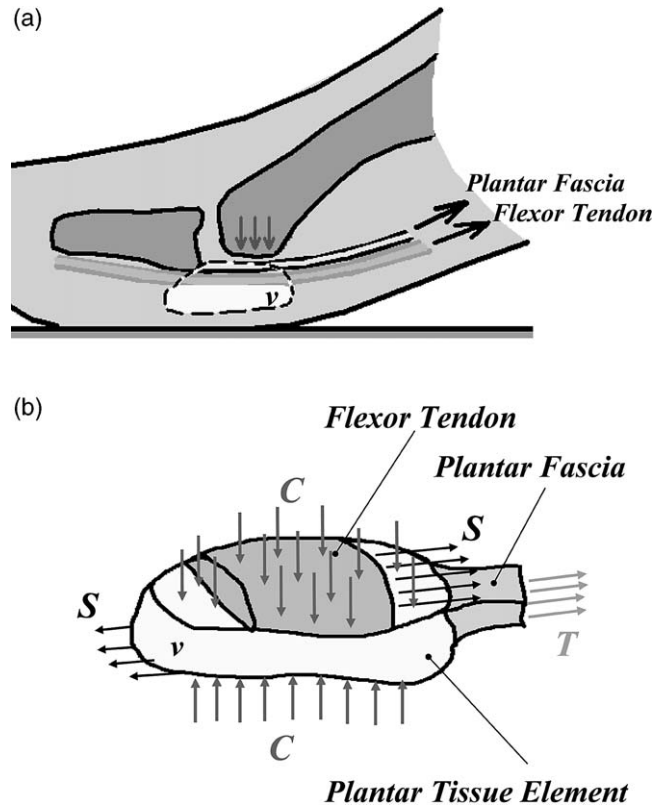
(a)



(b)



Fig. 6. Schematic description of the compound loading acting on the plantar tissue under the heads of the medial metatarsals during load bearing: (a) an element of soft tissue ($v$) underlying the head of the metatarsus is compressed between the bone and the shoe/ground. Simultaneously it is being subjected to tension and shear loading, applied by the stretched plantar fascia (and possibly by the flexor tendons that pass over the condyles of the metatarsal heads, with some intervention into adjacent soft tissue). (b) Consequently, element ($v$) is subjected to a system of compound mechanical stresses, including compression stress $C$, tension stress $T$ and shear stress $S$.

phase of gait, for evaluating the foot's main function of providing support during locomotion (see Ref. [30] for a review). Only a few studies have gathered static foot pressure data on a large, statistical scale to compare normal with abnormal foot-ground peak pressures.

Duckworth et al. [31] found that peak pressures in the normal foot during standing increase with age, and that they range from 61 to 108 KPa. Minns and Craxford [32] measured an average peak forefoot pressure of 79 KPa for 67 standing healthy subjects. Cavanagh et al. [33] analyzed 107 normal samples of pressure patterns during barefoot standing and found that the averaged normal peak pressures under the forefoot are 53 KPa. Taken together, these studies showed that average peak forefoot pressures under the apparently normal feet of healthy adults in the standing posture may range from 60 to 85 KPa. The present predictions of normal peak pressures under the medial metatarsals (55–66 KPa, Fig. 5a) are in good agreement with these experimental data.

The dominant characteristic of the pressure distribution under a diabetic foot is the appearance of sites of abnormally elevated pressures. These high-pressure sites, which are usually located under the forefoot, develop both while standing and during gait. A large-

group study by Duckworth et al. [15] analyzed foot-ground pressures under forefeet of 82 diabetic patients and reported an average peak forefoot pressure of 140 KPa. A more recent study by Kato et al. [34] similarly found that the averaged peak forefoot pressure in seven standing diabetics was 131 KPa. Thus, peak pressures under the medial metatarsal heads of diabetics during standing are about 1.5–2.3 times greater than normal. The present model predicts that in advanced stages of diabetes, contact pressures under the second metatarsal head during standing increase by a factor of 1.5 in respect to the normal condition (in agreement with the lower-end of the above range), and thus, the present predictions of internal stress distributions should be considered 'conservative'. These predictions show that an increase in a factor of 1.5 in contact stress is accompanied by an increase in a factor of 4.1 in average internal stresses. Therefore, it is very likely that the process of injury is not initiated on the skin surface but rather in deeper subcutaneous layers and in the tissues
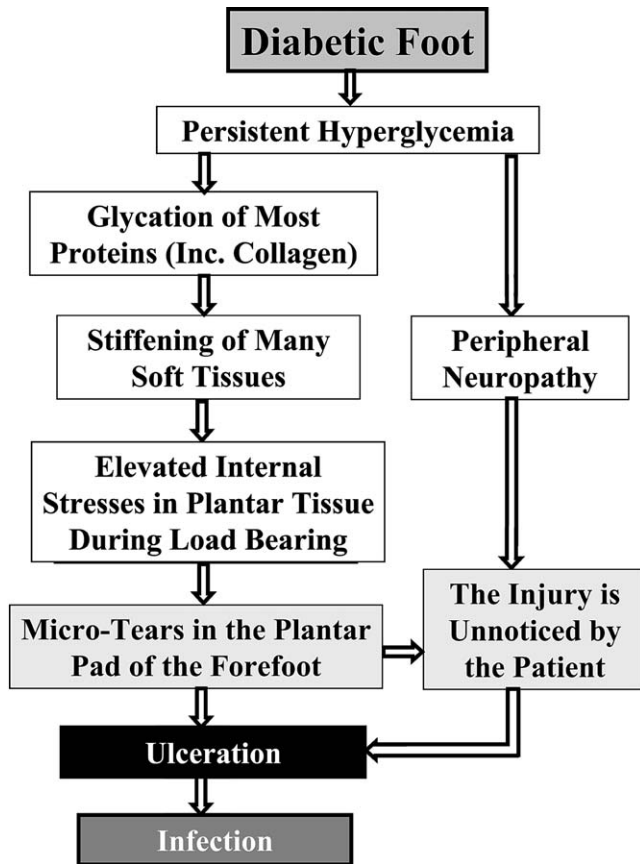
**Fig. 7.** The theory of ulceration of the diabetic foot: glycation-related stiffening of the plantar pad and consequent elevated stresses are the basic factors responsible for injury, which may progress unnoticeably due to peripheral neuropathy—a second effect of persistent hyperglycemia.

underlying the distal bony prominences of the metatarsals where abnormal stresses are more pronounced (Figs. 3 and 4).

The model employed for this study is based on several assumptions which should be taken into account while interpreting the results. First, for the purpose of modeling, the three-dimensional foot anatomy was represented as five planar sections. The inter-metatarsal ligaments that firmly hold the five rays of the foot and form an integral structure during standing allow the use of this approach: although the planar-section representation is not able to fully predict the spatial (out-of-plane) stress flow, it significantly simplifies the computational procedures compared with three-dimensional modeling [17,21]. Secondly, the plantar tissue is taken as a homogenous bulk (with the exception of inclusion of the plantar fascia), while it is really a more complex, multi-layered structure containing adipose, muscular and fibrous elements which interact in a variety of different ways. The plantar pad of the present model 'averages' the individual structural behaviours of each of these tissue components under load bearing. However, the global stress flow through the pad is not expected to be

significantly different in a more detailed model, since the elastic properties of fat and muscle tissue materials are around the same order of magnitude: for deformations of up to 20%, the elastic modulus of the lower limb muscles under passive uniaxial loading ranges from 100 to 250 KPa [35], and that of the fat tissue of the heel is around 100–300 KPa [12].

A third assumption concerns the representation of the development of diabetes: the simulations track progression of protein glycation within the plantar pad by stiffening its nonlinear elastic stress-strain relation, using the 'tissue stiffness ratio', $\kappa$. All simulations referred to the pre-ulceration condition in which integrity and material properties of the skeleton are unaffected [36] and there is no visible tissue degeneration. This approach was taken since about 35% of the diabetic patients who at some time develop ulceration have abnormally high-pressures at the ulcer sites before a visible evidence of injury actually appears [15,37,38]. Possible concurrent changes in foot positioning or skeletal/muscular loading due to neuropathy and improper proprioception, or due to voluntary/involuntary off-loading of part of the foot due to development of ulceration were not considered, since the individual foot function and postural response of diabetic neuropathic patients may vary considerably [39].

Applications of the model described herein may be broadened to investigate conservative or new surgical interventions for treating the diabetic foot and to evaluate their influence on the expected post-surgical foot-ground stress flow. Orthotics and supportive devices for the relief of contact pressure may also be assessed in order to assure that re-distribution of contact pressures is also accompanied by significant reduction of internal stresses under the metatarsal heads. Thus, in conjunction with plantar pressure measurements, computational foot modeling for analysis of internal (tissue) stresses shows great promise as being a highly effective tool in treatment planning. In the future, it is expected that three-dimensional biomechanical models of the musculoskeletal system and of the foot in particular will be produced directly from MRI/CT scans of individual patients, as a routine medical procedure. The attending medical staff would further be able to perform measurements of the plantar tissue's mechanical properties using ultrasound elastography or a similar noninvasive technique, and these data will be fed into the simulation to form a patient-specific, anatomically accurate computer model of the foot. The patient-specific model can then be used to enhance clinical prognosis, be an aid in prescription of special footwear, or even allow simulations of consequences of surgical procedures if such are needed, before they are implemented in the operating room.

## Acknowledgements

This study was supported by the Ela Kodesz Institute for Medical Engineering and Physical Sciences.

## References

[1] Dyck PJ, Giannini C. Pathologic alterations in the diabetic neuropathies of humans: a review. J Neuropathol Exp Neurol 1996;55:1181–93.

[2] Paterson RS. Management of diabetic and other high risk patients. In: Neale D, Adams I, editors. Common foot disorders. London: Churchill Livingstone; 1985. p. 171–83.

[3] Caputo GM, Cavanagh PR, Ulbrecht JS, Gibbons GW, Karchmer AW. Assessment and management of foot disease in patients with diabetes. N Engl J Med 1994;331:854–60.

[4] Grayson ML. Diabetic foot infections: antimicrobial therapy. Infect Dis Clin North Am 1995;9:143–60.

[5] Goodfield MJD, Millard LG. The skin in diabetes mellitus. Diabetologia 1988;31:567–75.

[6] Reihsner R, Menzel EJ. Two-dimensional stress-relaxation behavior of human skin as influenced by non-enzymatic glycation and the inhibitory agent aminoguanidine. J Biomech 1998;31:985–93.

[7] Cox NH, McCruden D, McQueen A, Jones SK, Ong-Tone L, Finlay AY, Frier BM. Histological findings in clinically normal skin of patients with insulin-dependent diabetes. Clin Exper Derm 1987;12:250–5.

[8] Hanna W, Friesen D, Bombardier C, Gladman D, Hanna A. Pathological features of thick skin. J Am Acad Derm 1987;16:546–53.

[9] Andreassen TT, Seyer-Hansen K, Oxlund HB. Biomechanical changes in connective tissues induced by experimental diabetes. Acta Endocrinol (Copenh) 1981;98:432–6.

[10] Jorgensen CS, Ahrensberg JM, Gregersen H, Flyvberg A. Tension-strain relations and morphometry of rat small intestine in experimental diabetes. Dig Dis Sci 2001;46:960–7.

[11] Cavanagh PR, Ulbrecht JS. Biomechanics of the foot in diabetes mellitus. In: Levin ME, O'Neal LW, Bowker JH, editors. The diabetic foot. Saint Louis, MO: Mosby; 1992. p. 199–232.

[12] Gefen A, Megido-Ravid M, Itzchak Y. In vivo biomechanical behavior of the human heel pad during the stance phase of gait. J Biomech 2001;34:1661–5.

[13] Gefen A, Megido-Ravid M, Azariah M, Itzchak Y, Arcan M. Integration of plantar soft tissue stiffness measurements in routine MRI of the diabetic foot. Clin Biomech 2001;16:921–5.

[14] Sammarco GJ. Biomechanics of the foot. In: Nordin M, Frankel VH, editors. Basic biomechanics of the musculoskeletal system. Philadelphia, PA: Lea & Febiger; 1989. p. 163–81.

[15] Duckworth T, Boulton AJM, Betts RP, Franks CI, Ward JD. Plantar pressure measurements and the prevention of ulceration in the diabetic foot. J Bone Joint Surg [Br] 1985;67:79–85.

[16] Payne C, Turner D, Miller K. Determinants of plantar pressures in the diabetic foot. J Diabetes Complications 2002;16:277–83.

[17] Gefen A, Megido-Ravid M, Itzchak Y, Arcan M. Biomechanical analysis of the three-dimensional foot structure during gait—a basic tool for clinical applications. J Biomech Eng 2000;122:630–9.

[18] Chu TM, Reddy NP, Padovan J. Three-dimensional finite element stress analysis of the polypropylene ankle-foot orthosis: static analysis. Med Eng Phys 1995;17:372–9.

[19] Patil KM, Braak LH, Huson A. Analysis of stresses in two-dimensional models of normal and neuropathic feet. Med Biol Eng Comput 1996;34:280–4.

[20] Lemmon D, Shiang TY, Hashmi A, Ulbrecht JS, Cavanagh PR. The effect of insoles in therapeutic footwear—a finite element approach. J Biomech 1997;30:615–20.

[21] Gefen A. Stress analysis of the standing foot following surgical plantar fascia release. J Biomech 2002;35:629–37.

[22] Nakamura S, Crowninshield RD, Cooper RR. An analysis of soft tissue loading in the foot: a preliminary report. Bull Prosth Res 1981;18:27–34.

[23] Race A, Amis AA. The mechanical properties of the two bundles of the human posterior cruciate ligament. J Biomech 1994;27:13–24.

[24] Siegler S, Block J, Schneck CD. The mechanical characteristics of the collateral ligaments of the human ankle joint. Foot Ankle 1988;8:234–42.

[25] Funk JR, Hall GW, Crandall JR, Pilkey WD. Linear and quasi-linear viscoelastic characterization of ankle ligaments. J Biomech Eng 2000;122:15–22.

[26] Simkin A. Structural analysis of the human foot in standing posture. Ph.D. Thesis, Tel Aviv University, Tel Aviv, Israel, 1982.

[27] Armstrong DG, Lavery LA, Bushman TR. Peak foot pressures influence the healing time of diabetic foot ulcers treated with total contact casts. J Rehabil Res Dev 1998;35:1–5.

[28] Lord M, Reynolds DP, Hughes JR. Foot pressure measurement: a review of clinical findings. J Biomed Eng 1986;8:283–94.

[29] Brash PD, Foster J, Vennart W, Anthony P, Tooke JE. Magnetic resonance imaging techniques demonstrate soft tissue damage in the diabetic foot. Diabet Med 1999;16:55–61.

[30] Cavanagh PR, Ulbrecht JS, Caputo GM. New developments in the biomechanics of the diabetic foot. Diabetes Metab Res Rev 2000;16:S6–S10.

[31] Duckworth T, Betts RP, Franks CI, Burke J. The measurement of pressures under the foot. Foot Ankle 1982;3:130–41.

[32] Minns RJ, Craxford AD. Pressure under the forefoot in rheumatoid arthritis. Clin Orthop Rel Res 1984;187:235–42.

[33] Cavanagh PR, Rodgers MM, Iiboshi A. Pressure distribution under symptom-free feet during barefoot standing. Foot Ankle 1987;7:262–76.

[34] Kato H, Takada T, Kawamura T, Hotta N, Torii S. The reduction and redistribution of plantar pressures using foot orthoses in diabetic patients. Diabetes Res Clin Pract 1996;31:115–8.

[35] Kovanen V, Suominen H, Heikkinen E. Mechanical properties of fast and slow skeletal muscle with special reference to collagen and endurance training. J Biomech 1984;17:725–35.

[36] Fleischli JG, Laughlin TJ, Lavery LA, Shah B, Lancot D, Agrawal CM, Athanasiou K. The effects of diabetes mellitus on the material properties of human metatarsal bones. J Foot Ankle Surg 1998;37:195–8.

[37] Veves A, Murray HJ, Young MJ, Boulton AJ. The risk of foot ulceration in diabetic patients with high foot pressure: a prospective study. Diabetologia 1992;35:660–3.

[38] Kastenbauer T, Sauseng S, Sokol G, Auinger M, Irsigler K. A prospective study of predictors for foot ulceration in type 2 diabetes. J Am Podiatr Med Assoc 2001;91:343–50.

[39] Sacco IC, Amadio AC. A study of biomechanical parameters in gait analysis and sensitive cronaxie of diabetic neuropathic patients. Clin Biomech 2000;15:196–202.